

FADS1 and the timing of human adaptation to agriculture

Sara Mathieson¹ & Iain Mathieson^{2*}

¹ Department of Computer Science, Swarthmore College, Swarthmore, PA 19081

² Department of Genetics, Perelman School of Medicine, University of Pennsylvania, Philadelphia PA 19104

* Correspondence to: mathi@penmedicine.upenn.edu

1 Abstract

2 Variation at the *FADS1/FADS2* gene cluster is functionally associated with differences in lipid
3 metabolism and is often hypothesized to reflect adaptation to an agricultural diet. Here, we test the
4 evidence for this relationship using both modern and ancient DNA data. We show that almost all the
5 inhabitants of Europe carried the ancestral allele until the derived allele was introduced approximately
6 8,500 years ago by Early Neolithic farming populations. However, we also show that it was not under
7 strong selection in these populations. We find that this allele, and other proposed agricultural adaptations
8 at *LCT/MCM6* and *SLC22A4*, were not strongly selected until much later, perhaps as late as the Bronze
9 Age. Similarly, increased copy number variation at the salivary amylase gene *AMY1* is not linked to the
10 development of agriculture although, in this case, the putative adaptation precedes the agricultural
11 transition. Our analysis shows that selection at the *FADS* locus was not tightly linked to the initial
12 introduction of agriculture and the Neolithic transition. Further, it suggests that the strongest signals of
13 recent human adaptation in Europe did not coincide with the Neolithic transition but with more recent
14 changes in environment, diet or efficiency of selection due to increases in effective population size.

15 Introduction

16 Human history has seen a number of major transitions in diet (Luca, et al. 2010). The most recent was the
17 transition to a modern “industrialized” diet based on intensive farming and highly processed food. Before
18 that, many parts of the world saw a dramatic transition from a diet based on hunting and gathering to a
19 diet heavily based on the products of agriculture. The transition occurred independently several times in
20 different parts of the world, but the earliest known example is the Fertile Crescent, at least 10,500 years
21 ago. From there agriculture spread gradually northwest through Anatolia into Europe, and eastwards to
22 the Indian subcontinent (Bellwood 2004). Even outside these periods of transition, differences in diet
23 based on both cultural preferences and food source availability would have been a major aspect of
24 environmental differences between human populations—differences that would likely lead to genetic
25 adaptation. Thus, by identifying and studying the evolution of genetic adaptations to diet, we learn not
26 only about historical changes in diet, but also about the genetic basis of diet-related phenotypic
27 differences among present-day human populations.

28
29 One previously identified adaptation involves the fatty acid desaturase genes *FADS1* and *FADS2*. These
30 genes encode proteins which catalyze key steps in the ω -3 and ω -6 lipid biosynthesis pathways
31 (Nakamura and Nara 2004). These pathways synthesize long-chain (LC) polyunsaturated fatty acids
32 (PUFA) necessary for cell- and, particularly, neuronal-membrane development from short-chain (SC)

33 PUFA (Darios and Davletov 2006). The evolutionary interaction with diet stems from the fact that
34 different diets contain different ratios of SC- and LC-PUFA. Specifically, diets that are high in meat or
35 marine products contain relatively high LC-PUFA levels, and thus may require lower levels of *FADS1*
36 and *FADS2* activity compared to diets that are high in plant-based fats (Ameur, et al. 2012; Mathias, et al.
37 2012; Fumagalli, et al. 2015; Kothapalli, et al. 2016; Buckley, et al. 2017; Ye, et al. 2017). As a result of
38 this environmental interaction, these genes have been repeatedly targeted by natural selection.

39
40 Most dramatically, a derived haplotype (“haplotype D”, following Ameur, et al. (2012)) containing the 3’
41 end of *FADS1* is at very high frequency in present-day African populations and intermediate to high
42 frequency in present-day Eurasians (Ameur, et al. 2012; Mathias, et al. 2012), and experienced ancient
43 positive selection in Africa (Ameur, et al. 2012; Mathias, et al. 2012). The derived haplotype increases
44 expression of *FADS1* (Ameur, et al. 2012) and likely represents an adaptation to a high ratio of SC- to
45 LC-PUFA, *i.e.* to a plant-based diet. In Europe, direct evidence from ancient DNA has shown that
46 haplotype D was rare around 10,000 years before present (BP) but has increased in frequency since then,
47 likely due to selection, to its present-day frequency of ~60% in Europe (Mathieson, et al. 2015). This
48 increase was plausibly associated with the adoption – starting around 8,500 BP in Southeastern Europe
49 before spreading North and West – of an agricultural lifestyle and diet that would have a higher SC- to
50 LC-PUFA ratio than the earlier hunter-gatherer diet (Mathieson, et al. 2015; Buckley, et al. 2017; Ye, et
51 al. 2017). Interestingly, the Altai Neanderthal genome shares at least a partial version of haplotype D
52 (Buckley, et al. 2017; Harris, et al. 2017), suggesting that the functional variation at this locus may
53 predate the split of Neanderthals and modern humans.

54
55 Other haplotypes at the locus have been shown to be under selection in different populations in more
56 recent history. In particular, another haplotype that is common in, but largely restricted to, the
57 Greenlandic Inuit population reduces the activity of *FADS1*, is associated with PUFA levels, and is likely
58 an adaptation to a diet that is extremely high in LC-PUFA from marine sources (Fumagalli, et al. 2015).
59 Conversely, a variant that increases expression of *FADS2* has been selected in South Asian populations –
60 and may be a specific adaptation to a vegetarian diet (Kothapalli, et al. 2016). Reflecting its important
61 role in lipid metabolism, variation at the *FADS* locus also contributes significantly to variation in lipid
62 levels in present-day populations. As well as directly contributing to variation in PUFA levels, SNPs in
63 haplotype D are among the strongest genome-wide association study (GWAS) signals for triglyceride and
64 cholesterol levels (Teslovich, et al. 2010). Thus, the complex evolutionary history of the region is not
65 only informative about ancient human diets, but also potentially relevant for understanding the
66 distribution of lipid-related disease risk both within and between populations. We therefore aimed to

67 characterize the history of the region, by combining inference from ancient and modern DNA data, in
68 order to understand the evolutionary basis of this important functional variation and its relationship with
69 changes in diet. We also compared the evolutionary history of the *FADS* locus with the histories of other
70 loci involved in dietary adaptation, to see whether we could detect shared patterns of adaptation.

71 Results

72 Haplotype structure at *FADS1*

73
74 We began by investigating 300 high-coverage whole-genome sequences from the Simons Genome
75 Diversity Project (SGDP) (Mallick, et al. 2016), as well as three archaic human genomes (Meyer, et al.
76 2012; Prufer, et al. 2014; Prufer, et al. 2017), to investigate the fine-scale haplotype structure in the region
77 (Figure 1, Supplementary Figure 1). By clustering haplotypes using a graph-adjacency algorithm
78 (Methods), we defined three nested “derived” haplotypes (Figure 1A, Table 1, Supplementary Table 1,
79 Supplementary Figure 1). Haplotype D extends over 78kb, is largely restricted to Eurasia, and is
80 comparable to the haplotype D defined by Aneur, et al. (2012). Haplotype C is an 18kb portion of
81 haplotype D that is shared between African and Eurasian populations. Finally, haplotype B is a 15kb
82 region that represents the portion of haplotype D that is shared between modern humans and both the
83 Altai (Prufer, et al. 2014) and Vindija (Prufer, et al. 2017) Neanderthals. We denote the modern human
84 haplotype carrying ancestral alleles at haplotype-defining SNPs as haplotype A (the “ancestral”
85 haplotype). This analysis also allows us to prioritize likely causal SNPs, which are currently unknown
86 (Buckley, et al. 2017; Ye, et al. 2017). If the derived SNP that was selected in modern humans was also
87 selected in Neanderthals, then it must lie in haplotype B, which is defined by just four SNPs (rs174546,
88 rs174547, rs174554 and rs174562).

89
90 Using data from the 1000 Genomes project (1000 Genomes Project Consortium 2015), we replicate the
91 observation (Mathias, et al. 2012; Buckley, et al. 2017; Harris, et al. 2017) that haplotypes in the
92 haplotype B region fall into two clusters (Figure 1B, Supplementary Figure 2). One cluster contains
93 Eurasian-ancestry individuals that carry haplotype A (and all individuals with Native American ancestry).
94 The other cluster contains Neanderthals, Eurasians that carry haplotype D, and almost all present-day
95 African-ancestry individuals. A small number of intermediate haplotypes are either recombinant or the
96 result of phasing errors. We inferred the phylogeny of the haplotype B region using BEAST2 (Figure 1C)
97 (Bouckaert, et al. 2014). The region is small and has a very low recombination rate, (average 0.03 cM/mb
98 according to the International HapMap Consortium (2007) combined recombination map), so we ignored
99 possible recombination events. Assuming that the common ancestor of human and chimp haplotypes was

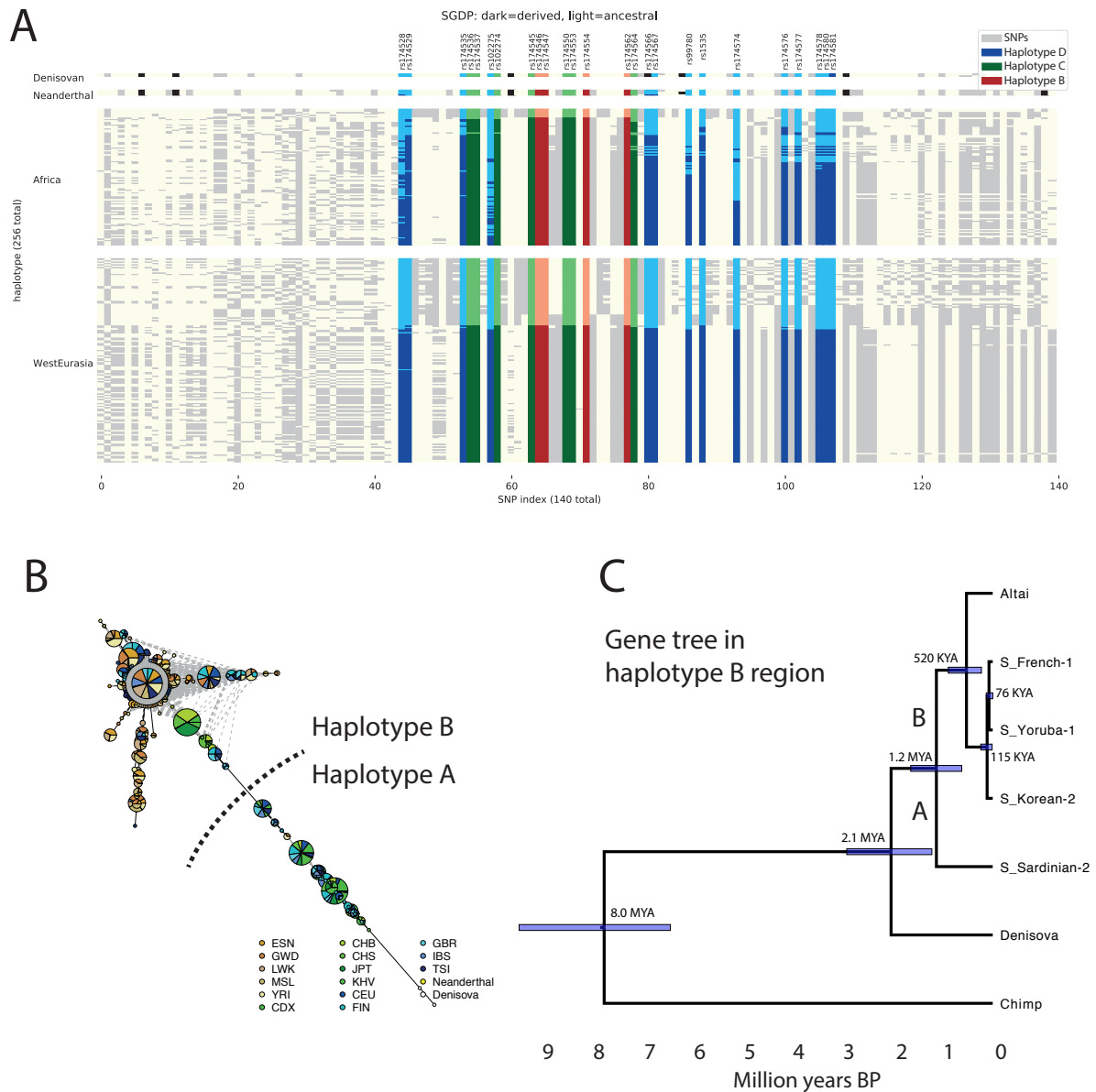


Figure 1: Haplotype structure at the *FADS1* region. **A:** Haplotypes from the SGDP African and West Eurasian populations (Mallick, et al. 2016) and the Neanderthal (Prufer, et al. 2014; Prufer, et al. 2017) and Denisovan (Meyer, et al. 2012) genomes. Each column represents a SNP and each row a phased haplotype. Dark and light colors represent derived and ancestral alleles at each SNP and blue, green and red colors indicate SNPs that are part of haplotypes D, C and B, respectively. **B:** Haplotype network for region B constructed from 1000 Genomes (1000 Genomes Project Consortium 2015) and archaic samples. Green, blue and brown indicate East Asian, European and African populations respectively. **C:** Gene tree for the haplotype B region inferred for representative haplotypes.

Haplotype	Length (kb)	State	Shared
A	-	Ancestral	-
B	15	Derived	Neanderthal and present-day humans
C	18	Derived	Present-day humans
D	78	Derived	Present-day Eurasians

Table 1: Haplotypes described in the text. Summary of the 4 haplotypes discussed. See Supplementary Table 1 for defining SNPs.

	P(New mut.)	Start (yrs BP)	Start CrI (yrs BP)	Sel. Coeff.
1. Selection for the derived allele in the ancestors of present-day Africans	0.74	310,548	202,409-492,231	0.001-0.002
2. Selection for the ancestral allele in the ancestors of present-day Europeans	0.25	246,399	49,358-1,137,909	0.000-0.028
3. Selection for the derived allele in Europe	0.00	2,538	1,695-4,048	0.034-0.069

Table 2: Summary of ABC results for three possible episodes of selection. We inferred the probability of selection on a new mutation (as opposed to standing variation), estimated selection-onset time, 95% credible intervals for this time, and 95% credible intervals for the selection coefficient. See Supplementary Tables 2 and 3 for more detailed results.

100 6.6-10.0 million years ago – corresponding to a genome-wide mutation rate of $\sim 4\text{-}6 \times 10^{-10}$ per-base per-
101 year (Amster and Sella 2016; Scally 2016) – we infer that the most recent common ancestor (MRCA) of
102 the present-day African (C) and European (D) haplotypes was around 76,000 BP, of haplotypes B and C
103 around 520,000 BP, and that of haplotypes A and B around 1.2 million BP. These dates are consistent
104 with the estimates of Harris, et al. (2017) and suggest that the European-specific haplotype D diverged
105 around the time of the out-of-Africa bottleneck and the diversification of non-African lineages (Mallick,
106 et al. 2016). They also suggest that modern human ancestral and derived haplotypes coexisted in the
107 Denisovan-Neanderthal-modern human ancestral population, with the Neanderthal haplotype splitting off
108 around the time of mean human-Neanderthal divergence 550-765,000 BP (Prufer, et al. 2014).

109

110 [ABC analysis of ancient selection in Africa and recent selection in Eurasia](#)

111

112 Having established the structure and phylogeny of the haplotypes in the region, we used approximate
113 Bayesian computation (ABC) (Wegmann, et al. 2010; Peter, et al. 2012) to infer the strength and timing
114 of selection on the derived haplotype in Africa (Table 1, Supplementary Table 2), first described by
115 Mathias, et al. (2012). Using data from the 1000 Genomes project, treating the derived allele of rs174546
116 as the selected SNP, and fixing the mutation rate to 1.25×10^{-8} per-base per-generation, we infer that
117 selection most likely but not definitively acted on a new mutation (posterior probability of new mutation
118 0.74, range 0.13-0.99, see Peter, et al. (2012) for details of the inference approach) and estimate that
119 selection began 202,000-492,000 BP (Supplementary Table 2). This estimates is uncertain though, with
120 95% credible intervals (CrIs) in different populations ranging from 84,000-1,426,000 BP. Mathias, et al.
121 (2012) estimated $85,000 \pm 84,000$ years for the onset of selection in Africa. However, that analysis
122 assumed a Human-Chimpanzee split of 6.5 million years, now thought to be an underestimate and, if
123 appropriately rescaled, would overlap the low end of our estimate. Overall, the evidence suggests that
124 selection began around or before the time of the deepest splits among human populations (Mallick, et al.
125 2016; Schlebusch, et al. 2017) 200,000-250,000 BP. This is consistent with the observation that the
126 derived allele is shared among all present-day African populations including those, such as Khoe-San and
127 Mbuti, which were substantially diverged from the ancestors of other present-day African populations at
128 least 100,000 BP (Mallick, et al. 2016; Schlebusch, et al. 2017).

129

130 In contrast, when we analyze present-day European genomes, we find that strong (selection coefficient
131 $s=3.4\text{-}6.9\%$) selection for the derived allele acted on standing variation (posterior probability=1.0) much
132 more recently – starting between 1700 and 4000 BP (95% CrIs in different populations range from 1000-
133 12,000 BP, Supplementary Table 2). This recent selection is hard to reconcile with the suggestion

134 (Mathieson, et al. 2015; Ye, et al. 2017) that it is closely linked to the development of agriculture, at least
135 10,500 BP (Bellwood 2004). It is also unclear why the derived haplotype was at such low frequency in
136 pre-agricultural Europeans (Mathieson, et al. 2015; Ye, et al. 2017), when ABC results and derived allele
137 sharing between African populations would imply that the derived allele would have been at high
138 frequency before the split of African and non-African ancestral populations. To resolve these questions,
139 we turned to ancient DNA data.

140

141 [Low frequency of the derived *FADS1* allele in Upper Palaeolithic Eurasia](#)

142

143 We first investigated why the derived haplotype was at such low frequency in pre-agricultural Europeans,
144 by analyzing data from 52 Paleolithic and Mesolithic individuals dated between 45,000 and 8,000 BP (Fu,
145 et al. 2014; Jones, et al. 2015; Fu, et al. 2016; Sikora, et al. 2017). We infer the presence of haplotype D
146 based on 5 SNPs that were typed on the “1240k” capture array used for most of these samples (Fu, et al.
147 2016). The derived haplotype is rare in all populations (Figure 2A, “Direct observations”). When we tried
148 to use imputation to increase sample size, the results were inconsistent. Specifically, imputed data
149 suggested a much higher frequency in most of the ancient population groupings, for example around 40%
150 frequency in the Vestonice population. This higher frequency agrees with a previous analysis of this data
151 by Ye, et al. (2017). However, we find that imputation is unreliable for these data because many of the Ice
152 Age samples have extremely low coverage. This leads to a high rate of false positive inference of the
153 derived allele because it is at relatively high frequency in the present-day populations used as a reference
154 panel. Older samples tend to have lower coverage and thus higher false positive rates, leading to a
155 spurious inference of a decline in frequency over time. We estimated the false positive rate as a function
156 of coverage by simulating low coverage data from present-day samples that carry the ancestral allele.
157 Non-zero derived allele frequency estimates in the imputed data are consistent with the estimated false
158 positive rate (Methods, Figure 2B). In fact, we find reliable evidence of the derived allele in only one
159 individual – from the 34,000 BP site of Sunghir (Sikora, et al. 2017). Therefore, it seems likely that the
160 derived allele was rare among early “out-of-Africa” populations, at least in Western Eurasia.

161

162 This lack of the derived allele in early non-Africans is surprising because our ABC analysis suggested
163 that selection within the ancestral population began at least 200,000 years ago, and the derived allele
164 would therefore be expected to have been at high frequency when African and non-African ancestors
165 diverged. Further, the derived allele is shared between present-day African populations that were
166 genetically isolated before the split of present-day African and non-African ancestors (Mallick, et al.
167 2016; Schlebusch, et al. 2017). Ye, et al. (2017) determined that the ancestral allele must have been

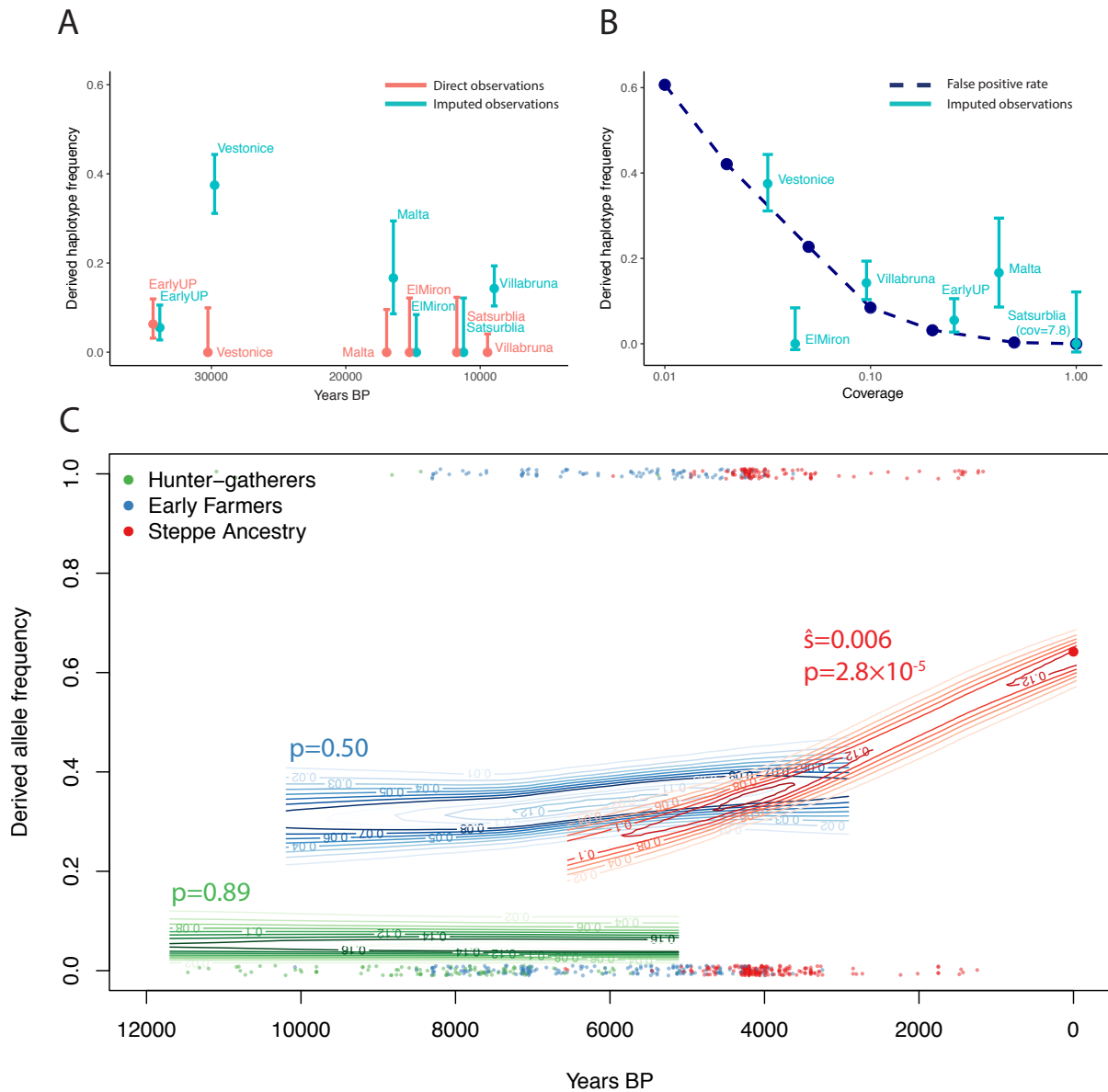


Figure 2: Direct ancient DNA evidence for the history of *FADS1*. **A:** Derived haplotype frequency estimated from direct observation of SNPs on the haplotype (red) and imputed data (blue) in Upper Palaeolithic individuals (45,000-10,000 BP) (Fu, et al. 2016). **B:** Estimated imputation false positive rate as a function of coverage (dashed line). Imputed allele frequencies in Upper Palaeolithic populations plotted for comparison at the median coverage in that population. **C:** Allele frequencies (at rs174546) over the past 12,000 years estimated from 1055 (669 with coverage) ancient and 99 modern individuals. Each point is an ancient pseudo-haploid individual call, at the bottom of the plot if it is ancestral and the top if it derived. Contours indicate the posterior probability of allele frequencies in the ancient populations and P-values for non-zero selection coefficients are indicated.

168 selected in the ancestors of present-day Europeans, but located this selection in Europe, after the out of
169 Africa bottleneck. Our analysis suggests that in fact, this selection was much older, occurring either
170 before or during the bottleneck. To test this, we used the same ABC approach we used to investigate the
171 derived allele to infer selection on the ancestral allele (Methods, Table 1, Supplementary Table 2). We
172 infer that the ancestral allele was selected from standing variation in the ancestors of present-day
173 Europeans ($s=0.1\%$, 95% CrI=0.0-2.8%), starting around 246,000 BP (95% CrI 49,000-1,138,000 BP).
174 This large credible interval overlaps the credible intervals for selection on the derived allele in African
175 ancestors and means that we do not have power to resolve these selective events. We also estimated the
176 timing of selection using an independent approach based on haplotype decay (Smith, et al. 2017),
177 qualitatively supporting ancient selection for the derived allele (Supplementary Table 4). These results
178 support the observation that if there was selection on the ancestral allele in the ancestors of present-day
179 Europeans, it occurred mostly before the date of the earliest ancient samples with genetic data.

180

181 Selection for the derived *FADS1* allele in Europe was not closely linked to early agriculture

182

183 The derived haplotype was almost absent in Upper Palaeolithic and Mesolithic Europe (before ~8,500
184 BP), but is today at a frequency of ~60%. Previous analysis of both ancient and modern DNA has inferred
185 strong selection for the allele over the past 10,000 years (Mathieson, et al. 2015; Field, et al. 2016;
186 Buckley, et al. 2017; Ye, et al. 2017). This has been interpreted to mean that selection for the derived
187 allele was driven by the development of agriculture, around 10,500 BP—a reasonable interpretation since
188 the derived allele is plausibly an adaption to a diet high in plant fats and low in animal fats. However, our
189 ABC analysis suggests that selection in Europe might actually be restricted to the past few thousand years
190 and thus post-date the development of agriculture by many millennia. To test this directly, we analyzed
191 data from 1055 ancient Europeans who lived between 12,000 and 1,000 BP (Keller, et al. 2012; Fu, et al.
192 2014; Gamba, et al. 2014; Lazaridis, et al. 2014; Olalde, et al. 2014; Raghavan, et al. 2014; Seguin-
193 Orlando, et al. 2014; Allentoft, et al. 2015; Gunther, et al. 2015; Haak, et al. 2015; Jones, et al. 2015;
194 Mathieson, et al. 2015; Cassidy, et al. 2016; Hofmanová, et al. 2016; Martiniano, et al. 2016; Schiffels, et
195 al. 2016; Jones, et al. 2017; Lazaridis, et al. 2017; Lipson, et al. 2017; Mathieson, et al. 2018; Olalde, et
196 al. 2018). We divided these individuals into three populations, based on their genome-wide ancestry
197 (Methods). First, individuals with “hunter-gatherer ancestry” were the Mesolithic inhabitants of Europe or
198 their descendants. Second, “Early Farmers” were people from Neolithic Northwest Anatolia or their
199 descendants, possibly admixed with hunter-gatherers, who migrated throughout Europe. Finally, people
200 with “Steppe ancestry” had ancestry that was originally derived from Bronze Age steppe populations like
201 the Yamnaya. (Lazaridis, et al. 2014; Allentoft, et al. 2015; Haak, et al. 2015). Because transitions

202 between these populations involved dramatic genetic discontinuity, with 75-100% of ancestry replaced
203 (Allentoft, et al. 2015; Haak, et al. 2015), we analyzed each of them separately.

204

205 In each of these three populations, we estimated the frequency and selection coefficient of the derived
206 allele by fitting a hidden Markov Model (HMM) to the time series of observations (Methods, Figure 2C)
207 (Mathieson and McVean 2013). We estimate that the selection coefficient in both hunter-gatherer and
208 Early Farmer populations was not significantly different from zero (i.e. no evidence that the allele was
209 under selection), and a selection coefficient of 0.6% (95% CI 0.4-1.5%) in Steppe-ancestry populations.
210 This selection coefficient is lower than that estimated using ABC. One possible explanation is that the
211 HMM forces the selection coefficient to be constant in each population, so if selection operated for only
212 part of the time represented, or in a subset of the population, its strength might be underestimated.
213 However, both the ancient DNA and ABC analyses are consistent with a relatively recent onset of
214 selection and show that, although the derived allele was present in early farming populations, it was not
215 strongly selected. Plausibly, the derived allele was introduced to the ancestors of the early farmers
216 through admixture with a population that carried “basal Eurasian” ancestry (Lazaridis, et al. 2016) not
217 found in Palaeolithic or Mesolithic Europe. Alternatively, the allele may have been retained in some,
218 unsampled, Upper Paleolithic Eurasian population, or driven to higher frequency somewhere by one or
219 more additional ancient episodes of selection.

220

221 Because agriculture was introduced to different parts of Europe at different times, spreading broadly from
222 south to north, we split the ancient DNA data into Northern and Southern European groups (Methods) and
223 re-ran the analysis, obtaining similar results in both groups (Supplementary Figure 3). To confirm the key
224 observation that the derived allele was not under selection in Early Farmers, we restricted to this group
225 and fitted a logistic regression to the observations with date, hunter-gatherer ancestry, Steppe ancestry and
226 latitude as covariates. None of these four coefficients were significantly different from zero ($P=0.19$, 0.89 ,
227 0.41 and 0.78 respectively), confirming that selection for the allele is not being masked by variation in
228 ancestry (for example by increasing hunter-gatherer ancestry over time), or in the geographic position of
229 sampled individuals (for example because agriculture began at different dates at different latitudes).
230 Finally, we split the Early Farmer and Steppe ancestry populations into 4000 year chunks and analyzed
231 them separately (Supplementary Figure 4). The frequency of the derived allele is higher in later Early
232 Farmers (after 6,000 BP), compared to early Early Farmers (40% vs 29%, Fisher’s exact test $P=0.026$),
233 perhaps reflecting a shift in ancestry. But we find no evidence of selection in either early or later Early
234 Farmers, or in early Steppe ancestry populations (before 4,000 BP).

235

236 Patterns of population differentiation at other lipid-associated alleles

237

238 SNPs that tag the derived haplotype are among the strongest genome-wide associations with lipid levels
239 (Teslovich, et al. 2010). To test whether the selective events we observe were consequences of more
240 general selection on lipid levels, we investigated patterns of African-European population differentiation
241 between variants associated with three blood lipid traits—triglycerides (TG), high-density cholesterol
242 (HDL) and low-density cholesterol (LDL) (Teslovich, et al. 2010). We find that, for HDL and TG, trait-
243 increasing alleles tend to be more common in African than European populations, while for LDL, the trait
244 increasing allele is more common in European populations (Figure 3A, Methods). These effects are in the
245 opposite direction to those of the *FADS1* haplotype. The derived allele, which is more common in African
246 than European populations, tends to decrease HDL and TG and increase LDL. We conclude that selection
247 on *FADS1* was not driven by its effect on overall blood lipid levels (which, if anything, moved in the
248 opposite direction), but by its specific effect on PUFA synthesis. We further find that there is no
249 significant difference in the frequency of LDL-increasing alleles when comparing the three ancient
250 populations (Figure 3B). Since they do differ in the frequency of the *FADS1* allele, this suggests that
251 recent selection on *FADS1* was also not driven by selection more generally on lipid levels.

252

253 Patterns of population differentiation at other diet-associated variants

254

255 We investigated whether other variants that have been suggested to be associated with the adoption of
256 agriculture showed similar temporal patterns of selection to *FADS1*. The salivary amylase gene *AMY1* is
257 highly copy-number variable among present-day populations, ranging from a diploid copy number of 2
258 (the ancestral state) to 17 (Groot, et al. 1991; Perry, et al. 2007; Usher, et al. 2015), with a mean of 6.7
259 copies in present-day Europeans (Usher, et al. 2015). It has been suggested that increased copy number
260 improves the digestion of starchy food and is therefore an adaptation to an agricultural diet that is
261 relatively rich in starch (Perry, et al. 2007). To date, one Early Farmer has been reported to have a
262 relatively high *AMY1* copy number of 16 (Lazaridis, et al. 2014), while six hunter-gatherers had 6-12
263 copies (Lazaridis, et al. 2014; Olalde, et al. 2014; Gunther, et al. 2018). Inchley, et al. (2016) showed that
264 the initial expansion of *AMY1* copy number predated the out-of-Africa bottleneck, and found no evidence
265 of recent selection. To investigate this directly, we called *AMY1* copy number in 76 ancient West
266 Eurasian individuals with published shotgun sequence data (Keller, et al. 2012; Meyer, et al. 2012;
267 Skoglund, et al. 2012; Gamba, et al. 2014; Lazaridis, et al. 2014; Olalde, et al. 2014; Prufer, et al. 2014;
268 Raghavan, et al. 2014; Skoglund, et al. 2014; Fu, et al. 2015; Gunther, et al. 2015; Cassidy, et al. 2016;
269 Kilinc, et al. 2016; Omrak, et al. 2016; Schiffels, et al. 2016; Prufer, et al. 2017; Saag, et al. 2017;
270 Gunther, et al. 2018). We counted the number of reads that mapped to regions around each of the three

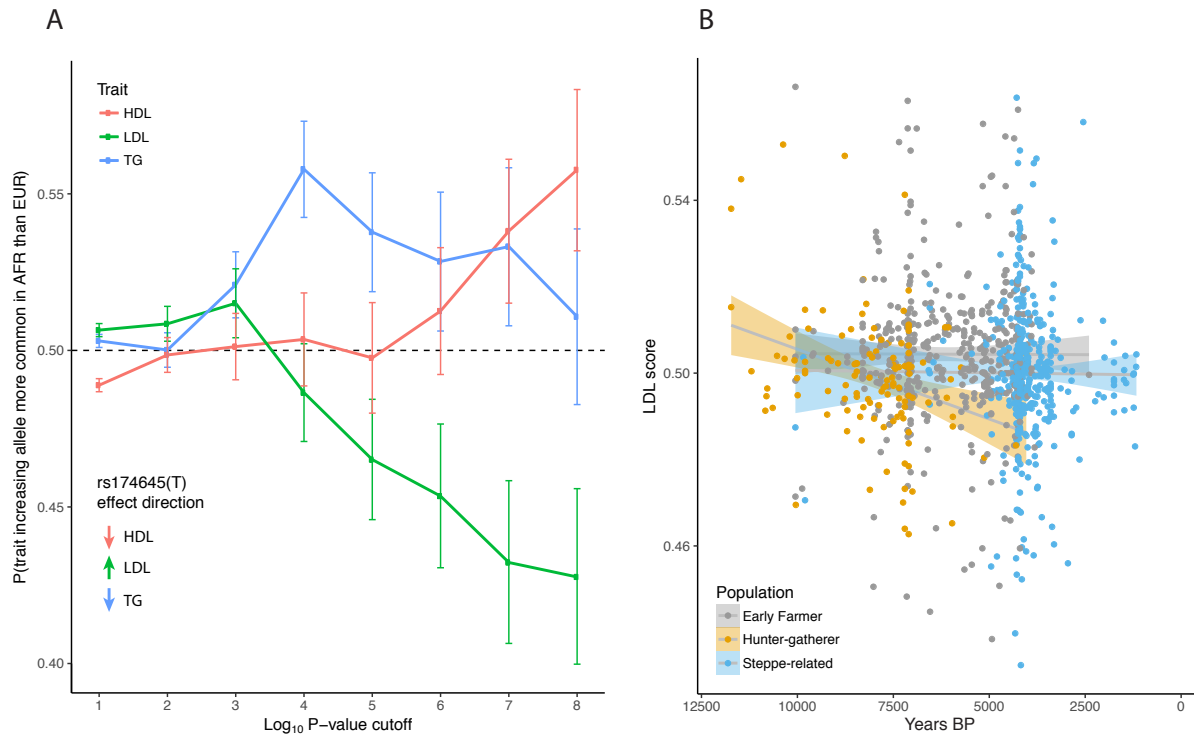


Figure 3: Trends in lipid-associated allele frequencies **A**: Probability that the trait-increasing allele is more common in African than European populations in the 1000 Genomes Project data (1000 Genomes Project Consortium 2015) for lipid-related traits. We show results for each trait with different P-value cutoffs. Vertical bars represent 95% confidence intervals. Inset shows the direction of effect for the derived FADS1 haplotype, using rs174546 as the tag SNP. **B**: LDL score for 1003 ancient individuals, classified according to ancestry, as a function of their age. LDL score is the proportion of significant LDL-associated variants at which the ancient individual carries the trait-increasing allele (Methods).

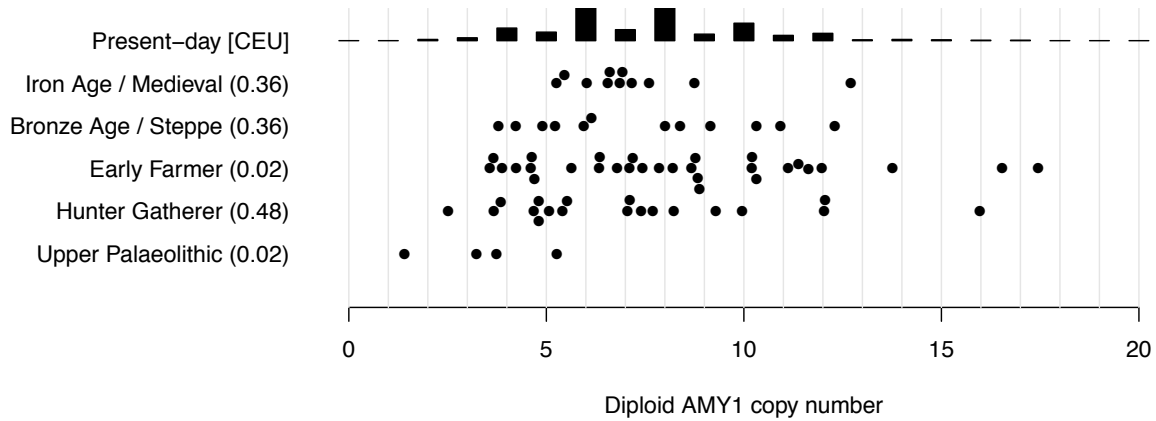


Figure 4: *AMY1* copy number. Inferred in ancient samples, arranged by time and subsistence strategy, compared with the distribution in a present-day population (CEU) with Northern European ancestry (Usher, et al. 2015). Parentheses: t-test P-values for difference between CEU and ancient populations.

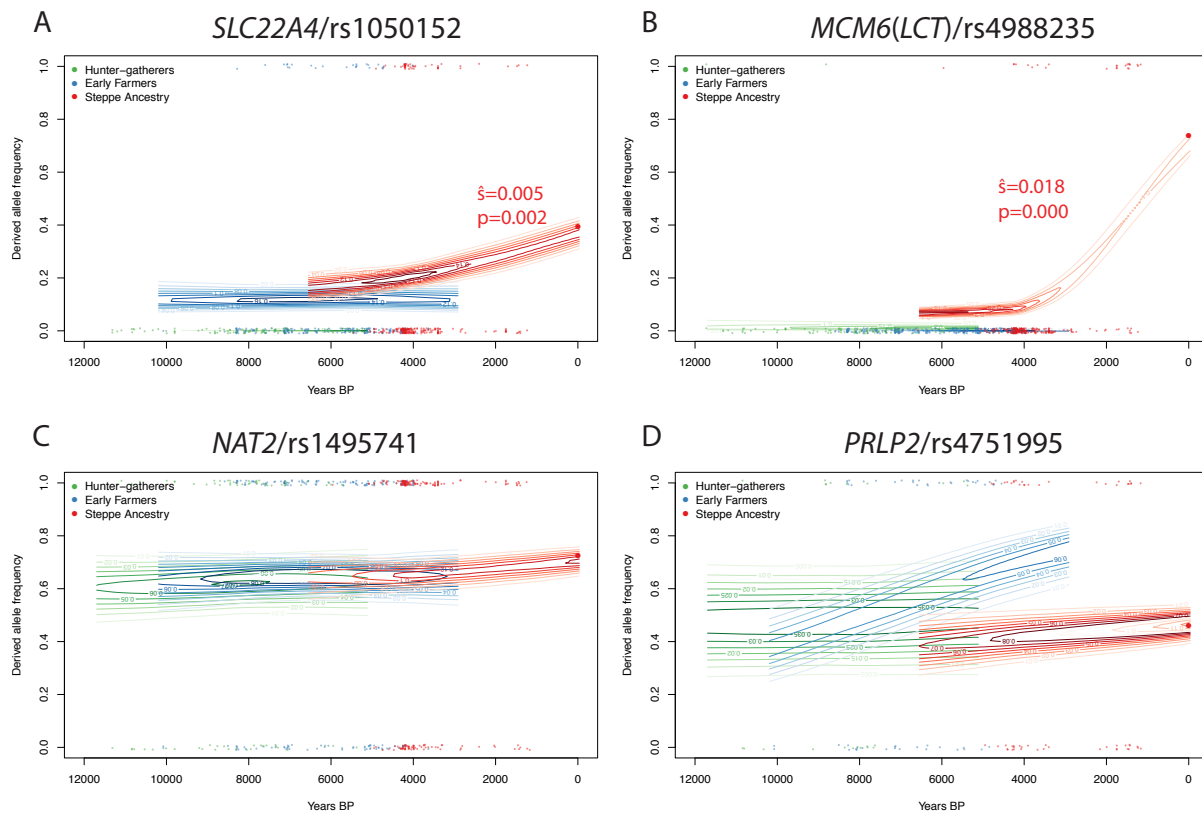


Figure 5: Allele frequency trajectories for other putative agricultural adaptation variants. As in Figure 2C, estimated allele frequency trajectories and selection coefficients in different ancient European populations. Significant selection coefficients are labelled.

271 *AMY1* copies in the human reference genome (Usher, et al. 2015), and compared to bootstrap estimates of
272 mean read depth with a linear correction for GC content (Methods, Figure 4, Supplementary Table 5). We
273 find no significant difference between *AMY1* copy number in present day Europeans and ancient
274 Europeans from the Iron Age/Medieval, Bronze Age, Neolithic, or Mesolithic periods. In particular,
275 Mesolithic pre-agricultural hunter-gatherers have a mean copy number of 7.2 – not statistically different
276 from present-day Europeans. Neolithic Early Farmers have a mean copy number of 8.4 – slightly higher,
277 but not significantly different (at a Bonferroni-corrected significance level of 0.01) from present-day
278 populations ($P=0.02$). We do find that four Upper Palaeolithic individuals dating between ~45,000-20,000
279 BP have lower *AMY1* copy number than present-day Europeans although, with a small sample size, this is
280 also not statistically significant (mean 3.4, $P=0.02$). These results therefore suggest an expansion in copy
281 number sometime earlier than ~10,000 BP and thus predating the development of agriculture.

282
283 Finally, we also investigated the history of other mutations that have been suggested to be involved in
284 adaptation to agricultural subsistence. It has been proposed, based on both ancient and modern DNA, that
285 the ergothioneine transporter gene *SLC22A4*—and in particular the nonsynonymous variant 503F
286 (rs1050152)—was targeted by selection in Early Neolithic farming populations (Huff, et al. 2012;
287 Mathieson, et al. 2015). However, analysis of our larger ancient DNA dataset reveals a more complicated
288 story, with an allele frequency trajectory similar to that of the *FADS1* derived allele (Figure 5A).
289 Specifically, the derived allele of rs1050152 is absent in hunter-gatherers, and present at low frequency in
290 Early Farmers and Bronze Age populations. But, similar to the derived *FADS1* allele, it does not increase
291 in frequency—and therefore does not appear to be under selection—in Early Farming populations. Strong
292 selection on this allele likely only operated in the past few thousand years. This timescale is similar to the
293 timescale over which the European lactase persistence variant (Enattah, et al. 2002) became common in
294 Europe (Figure 5B) (Burger, et al. 2007; Allentoft, et al. 2015; Mathieson, et al. 2015). The “slow
295 acetylator” variant of the *NAT2* gene has been hypothesized to be advantageous in agricultural
296 populations (Luca, et al. 2008; Magalon, et al. 2008; Sabbagh, et al. 2011). However, we find that a SNP
297 (rs1495741) that tags the “fast acetylator” phenotype (Garcia-Closas, et al. 2011) shows no change in
298 frequency over the past 10,000 years (Figure 5C). Finally, we find that a variant (rs4751995) in the gene
299 *PLRP2* that is relatively common in present-day populations with a cereal-based diet (Hancock, et al.
300 2010) is also more common in Early Farmers than hunter-gatherers, although it shows no evidence of
301 selection in any of these populations (Figure 5D).

302

303

304

305 Discussion

306

307 The combination of high-quality genome sequence data from present-day people, and large ancient DNA
308 datasets, provides new opportunities to investigate and understand the process of human adaptation. In
309 particular, the temporal aspect of ancient DNA data adds another dimension to our analysis, allowing us
310 to make precise inference of the timing of selection. We show that the derived allele was very rare or
311 absent in all European populations, until it was introduced around 8500 BP by migration from early
312 farmers carrying basal Eurasian ancestry. Although the derived allele is plausibly advantageous in
313 populations that consume a plant-based diet, we find no evidence that it was actually selected in early
314 European Farmers. Conversely, the low frequency of the derived allele in Upper Palaeolithic Europe is
315 consistent with isotopic evidence that protein intake was dominated by animal protein at this time
316 (Richards 2009). Finally, it is not known whether the Neanderthal allele would have had the same
317 function as the derived modern human allele. But if it did, it would not support the claim that the derived
318 allele is associated with a plant-based diet since Neanderthals, like Upper Palaeolithic modern humans,
319 are thought to have consumed a largely meat-based diet (Bocherens 2009). Therefore, the
320 derived/ancestral state at the major *FADS1* haplotype may not be a simple marker of plant- vs. meat-based
321 diet or more recent hunter-gatherer vs. farmer subsistence, but could reflect a more complex pattern of
322 interaction based on unknown dietary and genetic factors.

323

324 Our results support and extend several recent results about the evolutionary history of the *FADS1* allele. It
325 has previously been shown that the derived allele was anciently selected in Africa (Mathias, et al. 2012).
326 We find that the ancestral allele was rare in early non-African populations, suggesting that there may have
327 been selection for the ancestral allele as proposed by Ye, et al. (2017), but that it must have been before or
328 during—rather than after—the out-of-Africa bottleneck. The fixation of the ancestral allele in present-day
329 Native Americans has been interpreted as evidence for selection in their Siberian or Beringian ancestors
330 (Amorim, et al. 2017; Harris, et al. 2017; Hlusko, et al. 2018). However, our analysis shows that this may
331 not be the case, because the derived allele was likely very rare in Eurasia at the time of the Native
332 American-Eurasian split 20-25,000 BP (Raghavan, et al. 2015). Both Ye, et al. (2017) and Buckley, et al.
333 (2017) argue that recent selection in Europe for the derived allele was driven by changes in diet. Our
334 results support this view, with the caveat that the relevant changes were not simply those associated with
335 the Neolithic transition. Finally, Buckley, et al. (2017) found evidence for differential selective pressures
336 across Europe and propose the marker rs174594 as the target of selection. ABC analysis is consistent with
337 selection on rs174594 across Europe (Supplementary Table 6) but it is in strong LD with rs174546 and

338 we were unable to test the model of Buckley, et al. (2017) further because rs174594 is not on the capture
339 array that was used to generate most of the ancient DNA data we analyzed.

340
341 Similarly, due to limited ancient DNA data, we were not able to resolve the history of the *FADSI* allele in
342 East Asia. ABC analysis was very sensitive to the exact demography that we assumed. When we capped
343 recent N_e at 45,000, we found that the ancestral allele was selected in the ancestors of present-day East
344 Asians, although with a large credible interval (168,000-1,216,000 BP). The 39,000-year-old Tianyuan
345 individual did not carry the derived haplotype, further suggesting that it was absent in the Upper
346 Paleolithic ancestors of East Asians as well as Europeans. We estimated that the derived allele was
347 selected more anciently than in Europe (i.e. ~35,300 BP with 95% CrI 9,400-108,000 BP). The most
348 common East Asian derived haplotype is also an outgroup to the common European and African
349 haplotypes (Supplementary Figure 2), which would be consistent with deriving from a separate, older,
350 event. More ancient DNA from East Asia will help resolve this question, although we note that
351 agriculture developed later in East Asia than in Western Eurasia, so it is likely that selection on the
352 derived *FADSI* allele was also unassociated with the development of agriculture.

353
354 In the case of *FADSI* and all the other examples we investigated, the proposed agricultural adaption was
355 either not temporally linked with the initial development of agriculture or showed no evidence of
356 selection in Early Farmer populations. Instead, the three variants with any evidence of selection were
357 strongly selected at some point between the Bronze Age and the present day, that is, in the past ~4000
358 years. This time period is one in which there is relatively limited ancient DNA data, and so we are unable
359 to determine the timing of selection any more accurately. Future research should address the question of
360 why this recent time period saw the most rapid changes in apparently diet-associated genes. One plausible
361 hypothesis is that the change in environment or diet at this time was actually more dramatic than the
362 earlier change associated with the initial development agriculture. For example, Early Neolithic
363 populations may have retained some proportion of their diet from hunter-gatherer strategies, and only
364 later transitioned to a completely agricultural diet. Other environmental factors like pathogen load or
365 climate might also affect the selective pressures. Another hypothesis is that effective population sizes
366 were so small, or populations so structured, before the Bronze Age that selection did not operate
367 efficiently on variants with small selection coefficients. For example, analysis of present-day genomes
368 from the United Kingdom suggests that effective population size increased by a factor of 100-1000 in the
369 past 4500 years (Browning and Browning 2015). Larger ancient DNA datasets from the past 4,000 years
370 will likely resolve this question.

371 Materials and Methods

372

373 Identifying and analyzing *FADS1* haplotypes

374

375 We defined derived haplotypes using the following procedure. Within the region $\pm 50\text{kb}$ from rs174546
376 (hg19 chr11:61519830-61619830) there are 140 common ($\text{MAF} > 0.05$) SNPs when considering the
377 SGDP (600 haplotypes) and archaic (6 haplotypes) samples, and restricting to sites where the ancestral
378 allele can be determined based on the chimpanzee genome (PanTro2 Chimpanzee Sequencing Analysis
379 Consortium (2005)). For each pair of SNPs within these 140, we compute the number of “mismatches”
380 between ancestral and derived states. For example, if SNP 1 at haplotype H is in the ancestral state, but
381 SNP 2 at H is in the derived state, then this counts as one mismatch. 1000 Genomes data was used to set
382 the ancestral/derived state for each SNP (we used the chimpanzee allele if the allele was not present in
383 1000 Genomes). Counting up these mismatches for all pairs of SNPs, we obtain a 140×140 symmetric
384 “mismatch” matrix M . We transform this matrix into an “adjacency” matrix A by setting each entry to 1 if
385 the number of mismatches is below some threshold t , and 0 otherwise. In other words, if $M[i,j] \leq t$,
386 $A[i,j] = 1$, otherwise $A[i,j] = 0$. This adjacency matrix can then be interpreted as a graph, with SNPs as
387 the nodes and edges between SNPs if they are connected (i.e. have a low number of mismatches).

388

389 From this graph, we find the largest clique (connected component where every pair of nodes is
390 connected). This procedure can be interpreted as a way to find a subset of SNPs that are all in high LD
391 with each other. The problem of finding the largest clique in a graph is NP-hard, but we use the Bron-
392 Kerbosch algorithm which is more efficient in practice than brute force (Bron and Kerbosch 1973).

393

394 We use the procedure above to define 3 nested haplotypes: one considering all modern non-African
395 populations (haplotype D), one considering all modern human populations (haplotype C) and one
396 considering all modern and Neanderthal samples (haplotype B). For the mismatch thresholds, we use 12,
397 12, and 3 respectively (this last lower threshold accommodates the small sample size of archaic
398 populations). Haplotype D contains 25 SNPs, haplotype C contains 11 SNPs, and haplotype B 4 SNPs.

399 When there is more than one maximal clique of SNPs to choose from, we select one that is a subset of a
400 larger core. This means that haplotype B is a subset of haplotype C and haplotype C is a subset of
401 haplotype D. Note that our haplotype D differs slightly from the derived haplotype defined by Aneur, et
402 al. (2012) which was 28 SNPs long.

403

404 We constructed a haplotype network for the haplotype B region from 1000 Genomes European, East
405 Asian and African haplotypes, using the R package “pegas” (Paradis 2010). We inferred the phylogenetic
406 relationship between the haplotypes by picking a single individual from the SGDP that was homozygous
407 for each of the representative haplotypes and inferring the tree relating the haplotypes using BEAST2
408 (Bouckaert, et al. 2014). We rooted the tree with chimpanzee and used a uniform [6.6-10.0] million year
409 prior for human-chimp divergence. This corresponds to a genome-wide mutation rate of $\sim 4\text{-}6 \times 10^{-10}$ per-
410 base per-year.

411

412 ABC and startmrca analysis

413

414 To quantify the strength and timing of selection in different populations, we used approximate Bayesian
415 computation (ABC), implemented in the *ABCtoolbox* package (Wegmann, et al. 2010). We use the
416 pipeline implemented by Peter, et al. (2012), which uses a model selection approach to distinguish
417 selection on a *de novo* mutation (SDN) from selection on standing variation (SSV). Intuitively, this
418 approach simulates data under both the SDN and SSV models, for a range of parameters, and then selects
419 the simulations that best match the observed data, in the sense of being close in the space of a set of
420 predefined summary statistics. The parameters of the selected simulations are then used to estimate a
421 posterior distribution for the parameters of interest. In addition to SDN/SSV model selection, we
422 estimated two continuous parameters: the selection-onset time and the selection coefficient. To perform
423 the simulations for ABC we used *mbs* (Teshima and Innan 2009), which creates a selected allele
424 frequency trajectory backward in time from a specified present-day frequency. This implicitly creates a
425 range of selection-onset times in the past, which we used as a prior. For the selection strength, we used a
426 uniform prior of $[-4, -1]$ on the base-10 log of the selection coefficient.

427

428 We chose the derived allele (C) of rs174546 as the putatively selected allele, and analyzed 50kb on either
429 side for a total region length of $L=100\text{kb}$. We fixed the mutation rate at 1.25×10^{-8} per base per generation,
430 and used the recombination rate from the combined HapMap 2 map (International HapMap Consortium
431 2007). Since the recombination map may have changed over time, we also repeated the analysis using a
432 constant recombination rate of 1.1785×10^{-8} per base per generation (the average rate in this region). We
433 also set the current effective population size N_e to 10,000, and the heterozygote advantage at 0.5. This
434 mutation rate is at the low end of human mutation rate estimates (Sally 2016), but a higher mutation rate
435 would only lead to more recent estimates for the onset of selection. For each region (AFR, EAS, and
436 EUR) and each model (SDN and SSV), we simulated 1 million datasets. Each dataset had a sample size of
437 $n=170$ haplotypes and a length of $L=100\text{kb}$ to match the 1000 Genomes data. Within each region we

438 chose five representative populations for further analysis: ESN, GWD, LWK, MSL, and YRI for AFR;
439 CDX, CHB, CHS, JPT, and KHV for EAS; and CEU, FIN, GBR, IBS, and TSI for EUR. Based on the
440 current frequency of the selected allele in the subpopulations for each region, we computed simulation
441 priors: [0.984, 0.992] for AFR, [0.304, 0.670] for EAS, and [0.575, 0.699] for EUR. We also used
442 population-specific demographies from PSMC, based on Yoruba (AFR), Han (EAS), and French (EUR)
443 individuals from the SGDP (Mallick, et al. 2016).

444
445 For each simulated dataset we computed 27 summary statistics (as described in Peter, et al. (2012)).
446 During the ABC estimation phase, we retained the top 500 simulated datasets with statistics closest to
447 each real dataset (15 in total, one for each subpopulation), and computed posterior distributions for the
448 selection-onset time and selection coefficient. We computed combined estimates (Supplementary Table 2
449 and 3) by assuming a lognormal distribution for the posteriors and averaging over the five population-
450 specific estimates. Finally, we averaged over the two (SDN/SSV) model tested.

451
452 For EAS and EUR, we also wanted to test for ancient selection on the ancestral allele (T) of rs174546. To
453 this end, we merged the subpopulations for both EAS and EUR, and selected 295 haplotypes with the
454 ancestral allele for each. Then we ran our ABC procedure in the same way as before, except with a
455 “current” allele frequency of 0.999999 (*mbs* does not allow 1 for technical reasons). The EAS results
456 were very sensitive to demography—particularly to the value of present-day N_e —so we restricted maximum
457 N_e to the value of 45,000 used by Gravel, et al. (2011).

458
459 The main limitations of the ABC approach are that it does not model complex modes of selection and
460 relies on simulating under an appropriate range of parameters. We checked that ancient selection would
461 not obscure more recent signals of selection by simulating data under a realistic model of alternating
462 selection coefficients using *SLiM2* (Haller and Messer 2017), and rerunning the ABC analysis
463 (Supplementary Figure 5). Similarly, the results are conditional on simulating under the correct
464 demography and with an appropriate range of parameters. For our key results, we checked that the
465 distributions of simulated summary statistics were broadly consistent with the observed values, indicating
466 that our simulations are reasonable (Supplementary Figures 6-8). When we modeled selection on the
467 ancestral allele, we noticed that the observed values of the Fay and Wu H statistics were often outside the
468 simulated distribution (Supplementary Figure 7) – most likely because we flipped the selected allele – so
469 we excluded these four statistics from the ABC estimation for selection on the ancestral allele.

470

471 *Startmrca* (Smith, et al. 2017) is a method for estimating the selection-onset time of a beneficial allele. It
472 uses an HMM (in the “copying” style of Li and Stephens (2003)) to model present-day haplotypes as
473 imperfect mosaics of the selected haplotype and a reference panel of non-selected haplotypes. We used
474 this method to estimate the selection-onset time for the ancestral allele of rs174546 in the EAS and EUR
475 superpopulations described above. We used YRI individuals that are homozygous for the derived allele as
476 the reference panel. Following Smith, et al. (2017), we used a 1Mb region surrounding rs174546, the
477 HapMap combined recombination map in this region (International HapMap Consortium 2007), 100
478 haplotypes in the selected population, and 20 haplotypes in the reference population. To obtain selection-
479 onset time estimates for each population, we ran 5 independent MCMC chains, each with 10,000
480 iterations. We post-processed the results by discarding the first 6000 iterations (burn-in), and retaining the
481 remaining successful iterations over all 5 chains. To obtain credible intervals, we took the 2.5 and 97.5
482 quantiles of each resulting distribution (Supplementary Table 3.2).

483
484 We also analyzed selection for the derived allele of rs174546 in the EAS and EUR superpopulations. In
485 this case, there were not enough AFR individuals homozygous for the ancestral allele to use as a reference
486 population. So instead we used a “local” reference population, i.e. EAS and EUR individuals homozygous
487 for the ancestral allele. We also use a lower prior for the derived allele ([0-4,000] generations vs. [0-
488 20,000] for the ancestral). We did not analyze AFR because the selection is likely too old for the method,
489 and there is no suitable reference population. We note that *startmrca* tends to underestimate the time of
490 very ancient selective events (the “star” genealogy assumption becomes less appropriate). It also does not
491 account for selection on standing variation, which would result in an overestimation of the selection-onset
492 time, so our *startmrca* quantitative results are likely unreliable.

493

494 Ancient DNA analysis

495

496 We first analyzed 52 Palaeolithic and Mesolithic samples (Fu, et al. 2014; Jones, et al. 2015; Fu, et al.
497 2016; Sikora, et al. 2017) for the presence of the derived *FADS1* allele. These samples were typed on a
498 capture array (“1240k capture”) that contains 5 of the 25 SNPs that define haplotype D. We divided the
499 samples into population groups as defined by Fu, et al. (2016) and inferred the allele frequency in each of
500 these populations by maximizing the following likelihood function:

$$501 \sum_{i=1}^N \log \left(p^2 \prod_{j=1}^6 B(r_{ij}, r_{ij} + a_{ij}, \varepsilon) + 2p(1-p) \prod_{j=1}^6 B(r_{ij}, r_{ij} + a_{ij}, 0.5 + \delta) + (1-p)^2 \prod_{j=1}^6 B(r_{ij}, r_{ij} + a_{ij}, 1 - \gamma) \right)$$

502 where r_{ij} and a_{ij} are the number of reference and alternative reads from individual i at SNP j , N is the
503 number of individuals in the population. $B(x, n, p)$ is the binomial probability of seeing x successes out of n

504 trials with probability p , and $\varepsilon, \delta, \gamma$ are small error probabilities, which we set to 0.1, 0, 0.1 for
505 transversions, 0.15, 0.05, 0 for C>T or G>A transitions, and 0, 0.05, 0.15 for T>C or A>G transitions.
506 This implies a conservative 10% rate of contamination or error, and a 5% deamination rate. We computed
507 binomial confidence intervals assuming an effective sample size of $\sum_{i=1}^N \left\{ 2 - \left(\frac{1}{2} \right)^{\sum_{j=1}^5 (r_{ij} + a_{ij}) - 1} \right\}$.

508
509 To impute the *FADS1* haplotype in the Upper Palaeolithic and Mesolithic samples, we computed
510 genotype likelihoods at each typed SNP in the 5Mb region around rs174546, for each individual, assuming
511 a binomial distribution of reference and alternative allele counts and a 5% deamination rate. We then
512 imputed using *BEAGLE 4.1* (Browning and Browning 2016), and the 1000 Genomes reference panel
513 downloaded from bochet.gcc.biostat.washington.edu/beagle/1000_Genomes_phase3_v5a. We filtered out
514 imputed SNPs with a genotype probability of less than 0.8 and used the remaining SNPs to determine the
515 presence of the allele. In order to estimate the false positive rate, we simulated read data at different
516 coverages for 50 individuals from the 1000 Genomes EAS (East Asian) super-population who are
517 homozygous for the ancestral allele. We computed genotype likelihoods and imputed as for the ancient
518 data, having first removed the 50 test individuals from the reference panel. We performed 10 simulations
519 for each coverage level and used the frequency at which the derived allele was imputed as an estimate of
520 the false positive rate.

521
522 To analyze the Holocene history of *FADS1* and other alleles, we assembled a dataset of 1078 published
523 ancient samples, most of which were typed on the “1240k” capture array which targets ~1.24 million
524 SNPs. We used the pseudo-haploid version of these data, where each individual has a single allele at each
525 SNP, from a randomly selected read. We classified these individuals into “hunter-gatherer”, “Early
526 Farmer” and “Steppe ancestry” populations as follows. First, we ran supervised ADMIXTURE
527 (Alexander, et al. 2009) with $K=4$, and the four populations: WHG, EHG, Anatolia_Neolithic and
528 Yamnaya_Samara fixed to have cluster membership 1, as previously described (Mathieson, et al. 2018).
529 We then classified individuals based on their inferred ancestry. If they had more than 25% ancestry from
530 the Yamnaya_Samara cluster and dated later than 6000 BP, we classified them as “Steppe ancestry”. If
531 they had less than 25% ancestry from the Yamnaya_Samara cluster, more than 50% from the
532 Anatolia_Neolithic cluster and dated earlier than 2,000 BP, we classified them as “Early Farmer”. Finally,
533 if they had less than 25% ancestry from the Yamnaya_Samara cluster and less than 50% ancestry from
534 the Anatolia_Neolithic cluster and were dated earlier than 5100 BP, we classified them as “hunter-
535 gatherer”. We excluded 23 samples that did not fit into any of these classifications, leaving an analysis
536 dataset of 1055 samples of which 669 had coverage at rs174546. These classifications are informed by

537 previous analysis that combined genetic, chronological and archaeological information, and largely
538 correspond to classifications that would be derived from archaeological context alone. We estimated
539 allele frequency trajectories and selection coefficients separately for each population using a method that
540 fits a hidden Markov model to the observed frequencies (Mathieson and McVean 2013), assuming an
541 effective population size (N_e) of 10,000 in each population. We also analyzed separately the ancient
542 individuals from Northern and Southern Europe (Supplementary Figure 3). For this analysis, we defined
543 “Northern Europe” to be the region east of 13°E and north of 45°N, or west of 13°E and north of 49°N,
544 with “Southern Europe” as the complement. This corresponds approximately to the region reached by the
545 Neolithic transition by 7,000 BP (Fort 2015).

546
547 To call *AMY1* copy number we assembled a set of 76 ancient genomes with shotgun sequence data that
548 had nonzero mapped coverage at the locus. The majority of published ancient shotgun genomes have zero
549 coverage, presumably because the copy number variable region was masked during alignment. We
550 counted the number of reads that mapped to the any of the three *AMY1* duplicate regions in the human
551 reference genome (Usher, et al. 2015) and compared the total to the average read depth in 1000 random
552 regions of chromosome 1, of the same size as the *AMY1* duplicate regions. We fitted a linear model of
553 coverage as a function of GC content to these 1000 regions, for each individual, and used this to correct
554 our estimates for GC bias.

555

556 Analysis of lipid GWAS hits

557

558 We tested the directionality of lipid-associated alleles using genome-wide association meta-analysis
559 results for LDL, HDL and TG (Teslovich, et al. 2010). Specifically, we constructed a list of SNPs with P-
560 values below a given cutoff by iteratively selecting the SNP with the lowest P-value and then removing
561 all SNPs within 500kb. For each of these SNPs we extracted allele frequencies in the EUR and AFR
562 super-populations and then tested whether trait increasing alleles were more common in AFR than EUR
563 (Figure 3A).

564

565 To analyze the LDL hits in ancient samples, we first identified all SNPs with an association P-value less
566 than 10^{-6} that were on the capture array used to genotype the majority of the ancient samples. We
567 iteratively removed SNPs within 250kb of the most-associated SNPs to produce an independent set of
568 associated SNPs. For each (pseudo-haploid) individual, we constructed the “LDL score” by counting the
569 proportion of these SNPs at which that individual carried the trait-increasing allele (Figure 3B). We found
570 no significant differences with respect to ancestry when we fitted a binomial generalized linear model

571 with ancestry as a covariate. We also fitted a model including date as a covariate to test for significant
572 differences over time, also with a nonsignificant result.

573

574 Acknowledgments

575

576 We thank Rasmus Nielsen, Joshua Schraiber and two anonymous reviewers for helpful comments on an
577 earlier draft, and Benjamin Peter for help running the ABC methods.

578

579 References

580

581 1000 Genomes Project Consortium. 2015. A global reference for human genetic variation.
582 *Nature* 526:68-74.

583 Alexander DH, Novembre J, Lange K. 2009. Fast model-based estimation of ancestry in
584 unrelated individuals. *Genome Res* 19:1655-1664.

585 Allentoft ME, Sikora M, Sjogren KG, Rasmussen S, Rasmussen M, Stenderup J, Damgaard PB,
586 Schroeder H, Ahlstrom T, Vinner L, et al. 2015. Population genomics of Bronze Age Eurasia.
587 *Nature* 522:167-172.

588 Ameer A, Enroth S, Johansson A, Zaboli G, Igl W, Johansson AC, Rivas MA, Daly MJ, Schmitz
589 G, Hicks AA, et al. 2012. Genetic adaptation of fatty-acid metabolism: a human-specific
590 haplotype increasing the biosynthesis of long-chain omega-3 and omega-6 fatty acids. *Am J*
591 *Hum Genet* 90:809-820.

592 Amorim CE, Nunes K, Meyer D, Comas D, Bortolini MC, Salzano FM, Hunemeier T. 2017.
593 Genetic signature of natural selection in first Americans. *Proc Natl Acad Sci U S A* 114:2195-
594 2199.

595 Amster G, Sella G. 2016. Life history effects on the molecular clock of autosomes and sex
596 chromosomes. *Proc Natl Acad Sci U S A* 113:1588-1593.

597 Bellwood P. 2004. *First Farmers: The Origins of Agricultural Societies*: Wiley-Blackwell.

598 Bocherens H. 2009. Neanderthal Dietary Habits: Review of the Isotopic Evidence. In: Hublin J-
599 J, Richards MP, editors. *The Evolution of Hominin Diets*: Springer. p. 241-250.

600 Bouckaert R, Heled J, Kuhnert D, Vaughan T, Wu CH, Xie D, Suchard MA, Rambaut A,
601 Drummond AJ. 2014. BEAST 2: a software platform for Bayesian evolutionary analysis. *PLoS*
602 *Comput Biol* 10:e1003537.

603 Bron C, Kerbosch J. 1973. Finding All Cliques of an Undirected Graph [H]. *Communications of*
604 *the Acm* 16:575-577.

605 Browning BL, Browning SR. 2016. Genotype Imputation with Millions of Reference Samples.
606 *Am J Hum Genet* 98:116-126.

607 Browning SR, Browning BL. 2015. Accurate Non-parametric Estimation of Recent Effective
608 Population Size from Segments of Identity by Descent. *Am J Hum Genet* 97:404-418.

609 Buckley MT, Racimo F, Allentoft ME, Jensen MK, Jonsson A, Huang H, Hormozdiari F, Sikora
610 M, Marnetto D, Eskin E, et al. 2017. Selection in Europeans on Fatty Acid Desaturases
611 Associated with Dietary Changes. *Mol Biol Evol* 34:1307-1318.

- 612 Burger J, Kirchner M, Bramanti B, Haak W, Thomas MG. 2007. Absence of the lactase-
613 persistence-associated allele in early Neolithic Europeans. *Proc Natl Acad Sci U S A* 104:3736-
614 3741.
- 615 Cassidy LM, Martiniano R, Murphy EM, Teasdale MD, Mallory J, Hartwell B, Bradley DG.
616 2016. Neolithic and Bronze Age migration to Ireland and establishment of the insular Atlantic
617 genome. *Proceedings of the National Academy of Sciences* 113:368-373.
- 618 Chimpanzee Sequencing Analysis Consortium. 2005. Initial sequence of the chimpanzee genome
619 and comparison with the human genome. *Nature* 437:69-87.
- 620 Darios F, Davletov B. 2006. Omega-3 and omega-6 fatty acids stimulate cell membrane
621 expansion by acting on syntaxin 3. *Nature* 440:813-817.
- 622 Enattah NS, Sahi T, Savilahti E, Terwilliger JD, Peltonen L, Jarvela I. 2002. Identification of a
623 variant associated with adult-type hypolactasia. *Nat Genet* 30:233-237.
- 624 Field Y, Boyle EA, Telis N, Gao Z, Gaulton KJ, Golan D, Yengo L, Rocheleau G, Froguel P,
625 McCarthy MI, et al. 2016. Detection of human adaptation during the past 2000 years. *Science*
626 354:760-764.
- 627 Fort J. 2015. Demic and cultural diffusion propagated the Neolithic transition across different
628 regions of Europe. *J R Soc Interface* 12.
- 629 Fu Q, Hajdinjak M, Moldovan OT, Constantin S, Mallick S, Skoglund P, Patterson N, Rohland
630 N, Lazaridis I, Nickel B, et al. 2015. An early modern human from Romania with a recent
631 Neanderthal ancestor. *Nature* 524:216-219.
- 632 Fu Q, Li H, Moorjani P, Jay F, Slepchenko SM, Bondarev AA, Johnson PLF, Aximu-Petri A,
633 Prufer K, de Filippo C, et al. 2014. Genome sequence of a 45,000-year-old modern human from
634 western Siberia. *Nature* 514:445-449.
- 635 Fu Q, Posth C, Hajdinjak M, Petr M, Mallick S, Fernandes D, Furtwangler A, Haak W, Meyer
636 M, Mittnik A, et al. 2016. The genetic history of Ice Age Europe. *Nature* 534:200-205.
- 637 Fumagalli M, Moltke I, Grarup N, Racimo F, Bjerregaard P, Jorgensen ME, Korneliussen TS,
638 Gerbault P, Skotte L, Linneberg A, et al. 2015. Greenlandic Inuit show genetic signatures of diet
639 and climate adaptation. *Science* 349:1343-1347.
- 640 Gamba C, Jones ER, Teasdale MD, McLaughlin RL, Gonzalez-Fortes G, Mattiangeli V,
641 Domboróczki L, Kővári I, Pap I, Anders A, et al. 2014. Genome flux and stasis in a five
642 millennium transect of European prehistory. *Nat Commun* 5.
- 643 Garcia-Closas M, Hein DW, Silverman D, Malats N, Yeager M, Jacobs K, Doll MA, Figueroa
644 JD, Baris D, Schwenn M, et al. 2011. A single nucleotide polymorphism tags variation in the
645 arylamine N-acetyltransferase 2 phenotype in populations of European background.
646 *Pharmacogenet Genomics* 21:231-236.

- 647 Gravel S, Henn BM, Gutenkunst RN, Indap AR, Marth GT, Clark AG, Yu F, Gibbs RA,
648 Genomes P, Bustamante CD. 2011. Demographic history and rare allele sharing among human
649 populations. *Proc Natl Acad Sci U S A* 108:11983-11988.
- 650 Groot PC, Mager WH, Frants RR. 1991. Interpretation of polymorphic DNA patterns in the
651 human alpha-amylase multigene family. *Genomics* 10:779-785.
- 652 Gunther T, Malmstrom H, Svensson EM, Omrak A, Sanchez-Quinto F, Kilinc GM, Krzewinska
653 M, Eriksson G, Fraser M, Edlund H, et al. 2018. Population genomics of Mesolithic Scandinavia:
654 Investigating early postglacial migration routes and high-latitude adaptation. *PLoS Biol*
655 16:e2003703.
- 656 Gunther T, Valdiosera C, Malmstrom H, Urena I, Rodriguez-Varela R, Sverrisdottir OO,
657 Daskalaki EA, Skoglund P, Naidoo T, Svensson EM, et al. 2015. Ancient genomes link early
658 farmers from Atapuerca in Spain to modern-day Basques. *Proc Natl Acad Sci U S A* 112:11917-
659 11922.
- 660 Haak W, Lazaridis I, Patterson N, Rohland N, Mallick S, Llamas B, Brandt G, Nordenfelt S,
661 Harney E, Stewardson K, et al. 2015. Massive migration from the steppe was a source for Indo-
662 European languages in Europe. *Nature* 522:207-211.
- 663 Haller BC, Messer PW. 2017. SLiM 2: Flexible, Interactive Forward Genetic Simulations. *Mol*
664 *Biol Evol* 34:230-240.
- 665 Hancock AM, Witonsky DB, Ehler E, Alkorta-Aranburu G, Beall C, Gebremedhin A, Sukernik
666 R, Utermann G, Pritchard J, Coop G, et al. 2010. Human adaptations to diet, subsistence, and
667 ecoregion are due to subtle shifts in allele frequency. *Proc Natl Acad Sci U S A* 107 Suppl
668 2:8924-8930.
- 669 Harris DN, Ruczinski I, Yanek LR, Becker LC, Becker DM, Guio H, Cui T, Chilton FH, Mathias
670 RA, O'Connor T. 2017. Evolution of Hominin Polyunsaturated Fatty Acid Metabolism: From
671 Africa to the New World. *bioRxiv*:<https://doi.org/10.1101/175067>.
- 672 Hlusko LJ, Carlson JP, Chaplin G, Elias SA, Hoffecker JF, Huffman M, Jablonski NG, Monson
673 TA, O'Rourke DH, Pilloud MA, et al. 2018. Environmental selection during the last ice age on
674 the mother-to-infant transmission of vitamin D and fatty acids through breast milk. *Proc Natl*
675 *Acad Sci U S A*.
- 676 Hofmanová Z, Kreutzer S, Hellenthal G, Sell C, Diekmann Y, Diez-del-Molino D, van Dorp L,
677 López S, Kousathanas A, Link V, et al. 2016. Early farmers from across Europe directly
678 descended from Neolithic Aegeans. *Proceedings of the National Academy of Sciences* 113:6886-
679 6891.
- 680 Huff CD, Witherspoon DJ, Zhang Y, Gatenbee C, Denson LA, Kugathasan S, Hakonarson H,
681 Whiting A, Davis CT, Wu W, et al. 2012. Crohn's disease and genetic hitchhiking at IBD5. *Mol*
682 *Biol Evol* 29:101-111.

- 683 Inchley CE, Larbey CD, Shwan NA, Pagani L, Saag L, Antao T, Jacobs G, Hudjashov G,
684 Metspalu E, Mitt M, et al. 2016. Selective sweep on human amylase genes postdates the split
685 with Neanderthals. *Sci Rep* 6:37198.
- 686 International HapMap Consortium. 2007. A second generation human haplotype map of over 3.1
687 million SNPs. *Nature* 449:851-861.
- 688 Jones ER, Gonzalez-Fortes G, Connell S, Siska V, Eriksson A, Martiniano R, McLaughlin RL,
689 Llorente MG, Cassidy LM, Gamba C. 2015. Upper Palaeolithic genomes reveal deep roots of
690 modern Eurasians. *Nature communications* 6.
- 691 Jones ER, Zarina G, Moiseyev V, Lightfoot E, Nigst PR, Manica A, Pinhasi R, Bradley DG.
692 2017. The Neolithic Transition in the Baltic Was Not Driven by Admixture with Early European
693 Farmers. *Curr Biol* 27:576-582.
- 694 Keller A, Graefen A, Ball M, Matzas M, Boisguerin V, Maixner F, Leidinger P, Backes C,
695 Khairat R, Forster M, et al. 2012. New insights into the Tyrolean Iceman's origin and phenotype
696 as inferred by whole-genome sequencing. *Nat Commun* 3:698.
- 697 Kilinc GM, Omrak A, Ozer F, Gunther T, Buyukkarakaya AM, Bcakci E, Baird D, Donertas
698 HM, Ghalichi A, Yaka R, et al. 2016. The Demographic Development of the First Farmers in
699 Anatolia. *Curr Biol* 26:2659-2666.
- 700 Kothapalli KS, Ye K, Gadgil MS, Carlson SE, O'Brien KO, Zhang JY, Park HG, Ojukwu K, Zou
701 J, Hyon SS, et al. 2016. Positive Selection on a Regulatory Insertion-Deletion Polymorphism in
702 FADS2 Influences Apparent Endogenous Synthesis of Arachidonic Acid. *Mol Biol Evol*
703 33:1726-1739.
- 704 Lazaridis I, Mittnik A, Patterson N, Mallick S, Rohland N, Pfrengle S, Furtwängler A, Peltzer A,
705 Posth C, Vasilakis A, et al. 2017. Genetic origins of the Minoans and Mycenaeans. *Nature*
706 548:214-218.
- 707 Lazaridis I, Nadel D, Rollefson G, Merrett DC, Rohland N, Mallick S, Fernandes D, Novak M,
708 Gamarra B, Sirak K, et al. 2016. Genomic insights into the origin of farming in the ancient Near
709 East. *Nature* 536:419-424.
- 710 Lazaridis I, Patterson N, Mittnik A, Renaud G, Mallick S, Kirsanow K, Sudmant PH, Schraiber
711 JG, Castellano S, Lipson M, et al. 2014. Ancient human genomes suggest three ancestral
712 populations for present-day Europeans. *Nature* 513:409-413.
- 713 Li N, Stephens M. 2003. Modeling linkage disequilibrium and identifying recombination
714 hotspots using single-nucleotide polymorphism data. *Genetics* 165:2213-2233.
- 715 Lipson M, Szecsenyi-Nagy A, Mallick S, Posa A, Stegmar B, Keerl V, Rohland N, Stewardson
716 K, Ferry M, Michel M, et al. 2017. Parallel palaeogenomic transects reveal complex genetic
717 history of early European farmers. *Nature* 551:368-372.

- 718 Luca F, Bubba G, Basile M, Brdicka R, Michalodimitrakis E, Rickards O, Vershubsky G,
719 Quintana-Murci L, Kozlov AI, Novelletto A. 2008. Multiple advantageous amino acid variants in
720 the NAT2 gene in human populations. *PLoS One* 3:e3136.
- 721 Luca F, Perry GH, Di Rienzo A. 2010. Evolutionary adaptations to dietary changes. *Annu Rev*
722 *Nutr* 30:291-314.
- 723 Magalon H, Patin E, Austerlitz F, Hegay T, Aldashev A, Quintana-Murci L, Heyer E. 2008.
724 Population genetic diversity of the NAT2 gene supports a role of acetylation in human adaptation
725 to farming in Central Asia. *Eur J Hum Genet* 16:243-251.
- 726 Mallick S, Li H, Lipson M, Mathieson I, Gymrek M, Racimo F, Zhao M, Chennagiri N,
727 Nordenfelt S, Tandon A, et al. 2016. The Simons Genome Diversity Project: 300 genomes from
728 142 diverse populations. *Nature* 538:201-206.
- 729 Martiniano R, Caffell A, Holst M, Hunter-Mann K, Montgomery J, Müldner G, McLaughlin RL,
730 Teasdale MD, Van Rheezen W, Veldink JH. 2016. Genomic signals of migration and continuity
731 in Britain before the Anglo-Saxons. *Nature communications* 7:10326.
- 732 Mathias RA, Fu W, Akey JM, Ainsworth HC, Torgerson DG, Ruczinski I, Sergeant S, Barnes
733 KC, Chilton FH. 2012. Adaptive evolution of the FADS gene cluster within Africa. *PLoS One*
734 7:e44926.
- 735 Mathieson I, Alpaslan-Roodenberg S, Posth C, Szecsenyi-Nagy A, Rohland N, Mallick S, Olalde
736 I, Broomandkoshbacht N, Candilio F, Cheronet O, et al. 2018. The genomic history of
737 southeastern Europe. *Nature*.
- 738 Mathieson I, Lazaridis I, Rohland N, Mallick S, Patterson N, Roodenberg SA, Harney E,
739 Stewardson K, Fernandes D, Novak M, et al. 2015. Genome-wide patterns of selection in 230
740 ancient Eurasians. *Nature* 528:499-503.
- 741 Mathieson I, McVean G. 2013. Estimating selection coefficients in spatially structured
742 populations from time series data of allele frequencies. *Genetics* 193:973-984.
- 743 Meyer M, Kircher M, Gansauge MT, Li H, Racimo F, Mallick S, Schraiber JG, Jay F, Prufer K,
744 de Filippo C, et al. 2012. A high-coverage genome sequence from an archaic Denisovan
745 individual. *Science* 338:222-226.
- 746 Nakamura MT, Nara TY. 2004. Structure, function, and dietary regulation of delta6, delta5, and
747 delta9 desaturases. *Annu Rev Nutr* 24:345-376.
- 748 Olalde I, Allentoft ME, Sanchez-Quinto F, Santpere G, Chiang CW, DeGiorgio M, Prado-
749 Martinez J, Rodriguez JA, Rasmussen S, Quilez J, et al. 2014. Derived immune and ancestral
750 pigmentation alleles in a 7,000-year-old Mesolithic European. *Nature* 507:225-228.
- 751 Olalde I, Brace S, Allentoft ME, Armit I, Kristiansen K, Booth T, Rohland N, Mallick S,
752 Szecsenyi-Nagy A, Mittnik A, et al. 2018. The Beaker phenomenon and the genomic
753 transformation of northwest Europe. *Nature*.

- 754 Omrak A, Gunther T, Valdiosera C, Svensson EM, Malmstrom H, Kiesewetter H, Aylward W,
755 Stora J, Jakobsson M, Gotherstrom A. 2016. Genomic Evidence Establishes Anatolia as the
756 Source of the European Neolithic Gene Pool. *Curr Biol* 26:270-275.
- 757 Paradis E. 2010. pegas: an R package for population genetics with an integrated-modular
758 approach. *Bioinformatics* 26:419-420.
- 759 Perry GH, Dominy NJ, Claw KG, Lee AS, Fiegler H, Redon R, Werner J, Villanea FA,
760 Mountain JL, Misra R, et al. 2007. Diet and the evolution of human amylase gene copy number
761 variation. *Nat Genet* 39:1256-1260.
- 762 Peter BM, Huerta-Sanchez E, Nielsen R. 2012. Distinguishing between selective sweeps from
763 standing variation and from a de novo mutation. *PLoS Genet* 8:e1003011.
- 764 Prufer K, de Filippo C, Grote S, Mafessoni F, Korlevic P, Hajdinjak M, Vernot B, Skov L, Hsieh
765 P, Peyregne S, et al. 2017. A high-coverage Neandertal genome from Vindija Cave in Croatia.
766 *Science* 358:655-658.
- 767 Prufer K, Racimo F, Patterson N, Jay F, Sankararaman S, Sawyer S, Heinze A, Renaud G,
768 Sudmant PH, de Filippo C, et al. 2014. The complete genome sequence of a Neanderthal from
769 the Altai Mountains. *Nature* 505:43-49.
- 770 Raghavan M, Skoglund P, Graf KE, Metspalu M, Albrechtsen A, Moltke I, Rasmussen S,
771 Stafford Jr TW, Orlando L, Metspalu E, et al. 2014. Upper Palaeolithic Siberian genome reveals
772 dual ancestry of Native Americans. *Nature* 505:87-91.
- 773 Raghavan M, Steinrucken M, Harris K, Schiffels S, Rasmussen S, DeGiorgio M, Albrechtsen A,
774 Valdiosera C, Avila-Arcos MC, Malaspina AS, et al. 2015. Genomic evidence for the
775 Pleistocene and recent population history of Native Americans. *Science* 349:aab3884.
- 776 Richards MP. 2009. Stable Isotope Evidence for European Upper Paleolithic Human Diets. In:
777 Hublin J-J, Richards MP, editors. *The Evolution of Hominin Diets*: Springer. p. 251-257.
- 778 Saag L, Varul L, Scheib CL, Stenderup J, Allentoft ME, Saag L, Pagani L, Reidla M, Tambets
779 K, Metspalu E, et al. 2017. Extensive Farming in Estonia Started through a Sex-Biased
780 Migration from the Steppe. *Curr Biol* 27:2185-2193 e2186.
- 781 Sabbagh A, Darlu P, Crouau-Roy B, Poloni ES. 2011. Arylamine N-acetyltransferase 2 (NAT2)
782 genetic diversity and traditional subsistence: a worldwide population survey. *PLoS One*
783 6:e18507.
- 784 Scally A. 2016. The mutation rate in human evolution and demographic inference. *Curr Opin*
785 *Genet Dev* 41:36-43.
- 786 Schiffels S, Haak W, Paajanen P, Llamas B, Popescu E, Loe L, Clarke R, Lyons A, Mortimer R,
787 Sayer D. 2016. Iron age and Anglo-Saxon genomes from East England reveal British migration
788 history. *Nature communications* 7:10408.

- 789 Schlebusch CM, Malmstrom H, Gunther T, Sjodin P, Coutinho A, Edlund H, Munters AR,
790 Vicente M, Steyn M, Soodyall H, et al. 2017. Southern African ancient genomes estimate
791 modern human divergence to 350,000 to 260,000 years ago. *Science* 358:652-655.
- 792 Seguin-Orlando A, Korneliussen TS, Sikora M, Malaspina A-S, Manica A, Moltke I,
793 Albrechtsen A, Ko A, Margaryan A, Moiseyev V, et al. 2014. Genomic structure in Europeans
794 dating back at least 36,200 years. *Science* 346:1113-1118.
- 795 Sikora M, Seguin-Orlando A, Sousa VC, Albrechtsen A, Korneliussen T, Ko A, Rasmussen S,
796 Dupanloup I, Nigst PR, Bosch MD, et al. 2017. Ancient genomes show social and reproductive
797 behavior of early Upper Paleolithic foragers. *Science* 358:659-662.
- 798 Skoglund P, Malmstrom H, Omrak A, Raghavan M, Valdiosera C, Gunther T, Hall P, Tambets
799 K, Parik J, Sjogren KG, et al. 2014. Genomic diversity and admixture differs for Stone-Age
800 Scandinavian foragers and farmers. *Science* 344:747-750.
- 801 Skoglund P, Malmstrom H, Raghavan M, Stora J, Hall P, Willerslev E, Gilbert MT, Gotherstrom
802 A, Jakobsson M. 2012. Origins and genetic legacy of Neolithic farmers and hunter-gatherers in
803 Europe. *Science* 336:466-469.
- 804 Smith J, Coop G, Stephens M, Novembre J. 2017. Estimating Time to the Common Ancestor for
805 a Beneficial Allele. *Mol Biol Evol* 35:1003-1017.
- 806 Teshima KM, Innan H. 2009. mbs: modifying Hudson's ms software to generate samples of
807 DNA sequences with a biallelic site under selection. *BMC Bioinformatics* 10:166.
- 808 Teslovich TM, Musunuru K, Smith AV, Edmondson AC, Stylianou IM, Koseki M, Pirruccello
809 JP, Ripatti S, Chasman DI, Willer CJ, et al. 2010. Biological, clinical and population relevance
810 of 95 loci for blood lipids. *Nature* 466:707-713.
- 811 Usher CL, Handsaker RE, Esko T, Tuke MA, Weedon MN, Hastie AR, Cao H, Moon JE, Kashin
812 S, Fuchsberger C, et al. 2015. Structural forms of the human amylase locus and their
813 relationships to SNPs, haplotypes and obesity. *Nat Genet* 47:921-925.
- 814 Wegmann D, Leuenberger C, Neuenschwander S, Excoffier L. 2010. ABCtoolbox: a versatile
815 toolkit for approximate Bayesian computations. *BMC Bioinformatics* 11:116.
- 816 Ye K, Gao F, Wang D, Bar-Yosef O, Keinan A. 2017. Dietary adaptation of FADS genes in
817 Europe varied across time and geography. *Nat Ecol Evol* 1:167.
818
819